Electronic Supplementary Information

Solvent-modified porosity in chiral 3D kagome frameworks

Tony D. Keene,[ab] Damien Rankine,[a] Jack D. Evans,[a] Peter D. Southon,[c] Cameron J. Kepert,[c] Jade B. Aitken,[cde] Christopher J. Sumby*[a] and Christian J. Doonan*[a]

[a] *School of Chemistry and Physics, The University of Adelaide, SA 5005, Australia. CJD: Phone +61 8 8303 5770. Fax. +61 8 8303 4358. Email: christian.doonan@adelaide.edu.au; CJS: Phone +61 8 8303 7406. Fax. +61 8 8303 4358. Email: christopher.sumby@adelaide.edu.au*

[b] *Present address: School of Chemistry, University of Southampton, University Road, Southampton, SO17 1BJ, UK.*

[c] *School of Chemistry, The University of Sydney, NSW 2006, Australia.*

[d] *Institute of Materials Structure Science, KEK, Tsukuba, Ibaraki 305-0801, Japan.*

[e] *Australian Synchrotron, Clayton, Victoria, 3168, Australia,*

Contents

1. General Experimental

^1H and ^{13}C NMR spectra were recorded on a Varian Gemini spectrometer operating at 300 MHz and 80 MHz, respectively. ^1H and ^{13}C Spectra were referenced to 7.26 ppm and 77.0 ppm in $CDCl_3$ and 2.50 ppm and 39.6 ppm in DMSO-d_6, respectively. Melting points were recorded on a Reichert electrothermal melting point apparatus and are uncorrected. The Campbell microanalytical laboratory at the University of Otago, Dunedin performed all elemental analyses. Electrospray Ionisation-Mass Spectrometry (ESI-MS) was performed on a Finnigan LCQ mass spectrometer. Infrared (IR) spectra were recorded on a Perkin−Elmer Fourier Transform Infrared (FT−IR) spectrometer on a zinc−selenide crystal.

Thermogravimetric analysis (TGA) was performed on a Perkin−Elmer STA-6000 under a constant flow of N_2 (20 L/min) at a temperature ramp rate of 5°C/min. Water cycling TGA experiments were performed using an Ar flow saturated with H_2O (20 L/min) during isothermal stages at room temperature and a N_2 flow (20 L/min) during all other stages.

N_2 adsorption isotherms at 77 K were recorded on a Micromeritics ASAP 2020 adsorption analyser. The Braunner-Emmett-Teller (BET) method[1] was used for determining surface areas from N_2 isotherms at 77 K and further validated using the method of Walton and Snurr.[2] Pore size distribution plots were calculated from N_2 isotherms at 77 K using the DFT method and the Zeolite 13X model, through the Micromeritics ASAP 2020 software.

2. Synthetic Procedures

Dimethyl 2,2'-dimethoxy-1,1'-biphenyl-4,4'-dicarboxylate (**3**) was synthesised using literature procedures.[3] **4** and **H_4diol** were synthesised using the conditions shown below.

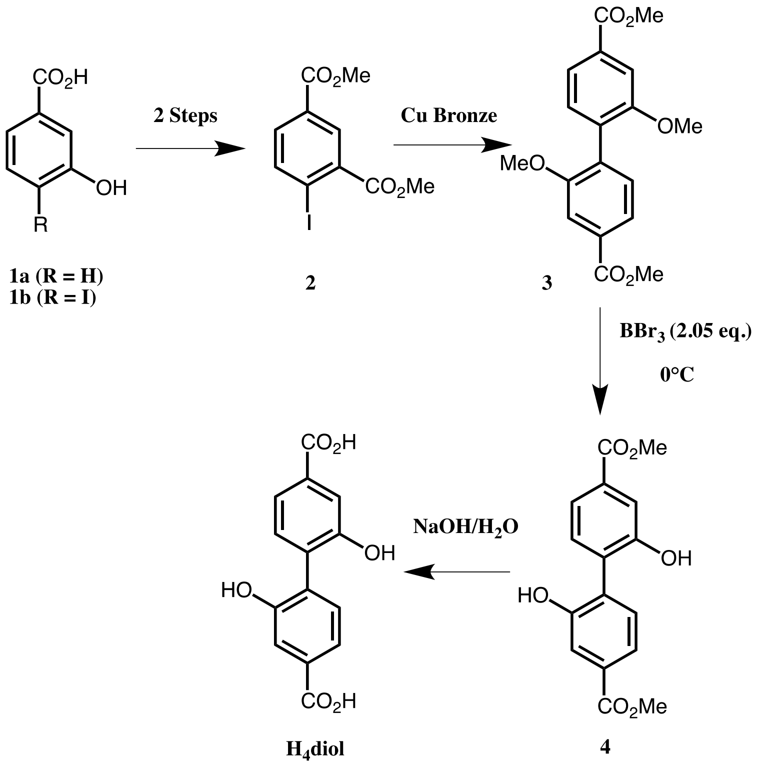

Scheme S1. Synthesis of **H_4diol** from 3-hydroxybenzoic acid.

Dimethyl 2,2'-dihydroxy-1,1'-biphenyl-4,4'-dicarboxylate (**4**)

To a solution of dimethyl 2,2'-dimethoxy-1,1'-biphenyl-4,4'-dicarboxylate (**3**) (1.33 g, 4.0mmol) in dry CH_2Cl_2 (60 mL) at 0°C, was added a solution of BBr_3 (0.77 mL, 8.0mmol) in dry CH_2Cl_2 (10 mL), dropwise over 20 minutes, under Ar atmosphere. The resulting orange solution was stirred at 0°C for 2 hours and then at room temperature for 2 hours. EtOH (2 mL) was then added dropwise followed by H_2O (50 mL) and stirred for 15 minutes. The resulting suspension was separated and the aqueous layer extracted with DCM (50 mL). The combined DCM extracts were discarded and the aqueous solution extracted with EtOAc (4 x 50 mL). The combined EtOAc extracts were washed with water (50 mL) and brine (80 mL), dried over $MgSO_4$ and filtered to a pale yellow solution. The solvent was evaporated under reduced pressure and dried *in vacuo* to give a colourless solid of dimethyl 2,2'-dihydroxy-1,1'-biphenyl-4,4'-dicarboxylate (**4**) (1.05 g, 87%). ^{1}H NMR (d^6-DMSO, 200MHz): δ 7.43 (s, 2H), 7.37 (dd, J = 1.4, 8.0 Hz, 2H), 7.32 (d, J = 8.0 Hz, 2H), 3.84 (s, 6H).

*2,2'-Dihydroxy-1,1'-biphenyl-4,4'-dicarboxylic acid (**H_4diol**)*

To a solution of dimethyl 2,2'-dihydroxy-1,1'-biphenyl-4,4'-dicarboxylate (**4**) (1.05 g, 3.48mmol) in THF (40 mL) and MeOH (4 mL) was added a 3.0M aqueous NaOH solution (10 mL) and the resulting mixture stirred at room temperature overnight. THF was evaporated *in vacuo* and the solution cooled to 0°C before acidifying to pH 1 with conc. aqueous HCl solution. The precipitate was collected via filtration, washing with H_2O, and dried via azeotropic distillation (toluene) to give a colourless solid of 2,2'-dihydroxy-1,1'-biphenyl-4,4'-dicarboxylic acid (**H_4diol**) (0.93 g, 98%) M.p. >360°C (decomp.);^{1}H NMR (d^6-DMSO, 200MHz): δ 12.80 (br. s, 2H), 9.75 (br. s, 2H), 7.50 (d, J = 1.4 Hz, 2H), 7.41 (dd, J = 1.6, 7.8 Hz, 2H), 7.26 (d, J = 7.8 Hz, 2H); ^{13}C NMR (d^6-DMSO, 50 MHz): δ 167.13, 154.53, 131.28, 130.88, 119.57, 116.26, 82.01.

3. MOF Synthesis and Activation Conditions

Synthesis

[Ni(H_2diol)(DMF)$_2$]·DMF: H_4diol (27.3 mg, 0.1 mmol) and $Ni(NO_3)_2.6H_2O$ (29.1 mg, 0.1 mmol) were dissolved in DMF (2.0 mL) and to this solution was slowly added DABCO (1.0 mL, 0.1 M DMF solution). The resulting mixture was sealed in a 5 mL teflon-lined steel pressure vessel and heated at 100 °C for 6 hours to yield green crystals of **[Ni(H_2diol)(DMF)$_2$]·DMF** in ~ 50 % yield. Analysis calc. for [**Ni(H_2diol)(DMF)$_2$]·DCM**: C 47.76, H 4.21, N 5.31; Found C 48.33, H 4.76, N 4.82%.

[Ni(H_2diol)(DEF)$_2$]·⅓DEF: H_4diol (27.3 mg, 0.1 mmol) and $Ni(NO_3)_2.6H_2O$ (29.1 mg, 0.1 mmol) were dissolved in DEF (2.0 mL) and to this solution was slowly added DABCO (1.0 mL, 0.1 M DEF solution). The resulting mixture was sealed in a 5 mL teflon-lined steel pressure vessel and heated at 100 °C for 6 hours to yield green crystals of **[Ni(H_2diol)(DEF)$_2$]·⅓DEF** in ~ 50 % yield. Analysis calc. for [**Ni(H_2diol)(DEF)$_2$]·H_2O**: C 52.48, H 5.52, N 5.10; Found C 52.57, H 5.44, N 4.82%.

Activation

[Ni(H_2diol)(DMF)$_2$] and **[Ni(H_2diol)(DEF)$_2$]** were prepared by washing with 4 × 3 mL DMF (for **[Ni(H_2diol)(DMF)$_2$]**) or DEF (for **[Ni(H_2diol)(DEF)$_2$]**) and then soaked for 4-5 hours in 3 mL of the same solvent. Samples were then exchanged with 4 × 3 mL CH_2Cl_2 for 2-3 hours. Excess liquid CH_2Cl_2 was extracted and the sample was dried briefly under a flow of N_2 before placing under vacuum overnight at ~3 μbar. Samples were then heated to 50 °C at 3 μbar for 4 hours prior to gas adsorption measurements.

[**Ni(H_2diol)]** was prepared by washing with DMF as above and then with 4 × 3 mL MeOH over 5 hours, followed by 1 × 10 mL MeOH overnight. Samples were then heated at 90°C at 3 μbar overnight prior to gas adsorption measurements.

4. X-Ray Diffraction Methods and Crystallographic Data

i. General Methods

Crystals were mounted under paratone oil on a plastic loop. X-ray diffraction data were collected with Mo-Kα radiation (λ = 0.7107 Å) using Oxford Diffraction X-calibur single crystal X-ray diffractometer at 150(2) K. Data sets were corrected for absorption using a multi-scan method, and structures were solved by direct methods using SHELXS-97[4] and refined by full-matrix least squares on F^2 by SHELXL-86,[5] interfaced through the program WinGX.[6] In general, all non-hydrogen atoms were refined anisotropically and hydrogen atoms were included as invariants at geometrically estimated positions, unless specified otherwise in additional details below. Details of data collections and structure refinements are given below. CCDC 915130 and 915131 contain the supplementary crystallographic data for these structures. These data can be obtained free of charge from The Cambridge Crystallographic Data Centre via www.ccdc.cam.ac.uk/data_request/cif. A summary of the crystallographic data and structure refinements are given in Tables S1 – S3.

In-house powder X-ray diffraction (PXRD) data was collected on a Rigaku Hiflux Homelab system using Cu-Kα radiation with an R-Axis IV++ image plate detector. Samples were mounted on plastic loops using paratone-N and data collected by scanning 90° in phi for 120 second exposures. The data was converted into *xye* format using the program DataSqueeze. Simulated powder X-ray diffraction patterns were generated from the single crystal data using Mercury 2.3. Le Bail refinement of PXRD patterns was performed in Rietica. Variable-temperature powder X-ray diffraction was collected on the PD beamline at the Australian Synchrotron at an energy of 15keV. Data was merged using the program DataPro.

ii. Single crystal X-ray diffraction

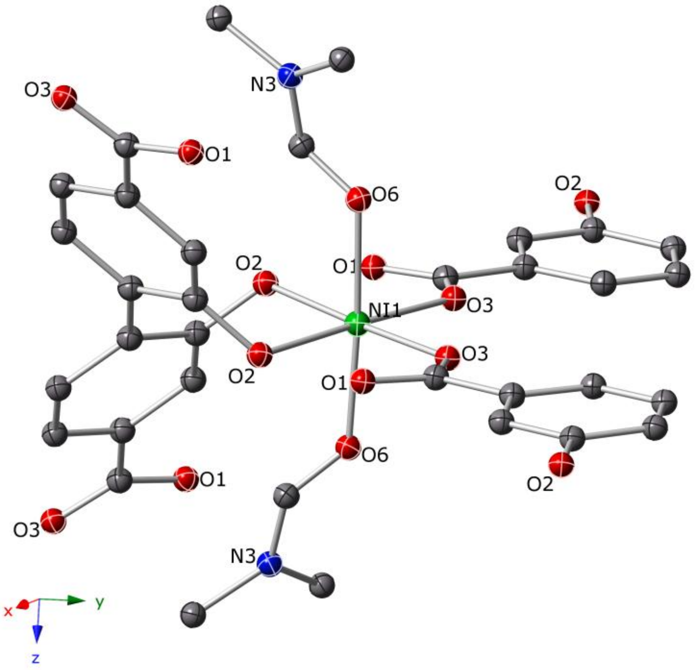

Figure S4.1. Coordination environment around the Ni(II) centre in **[Ni(H$_2$diol)(DMF)$_2$]**. Hydrogen atoms have been omitted for clarity.

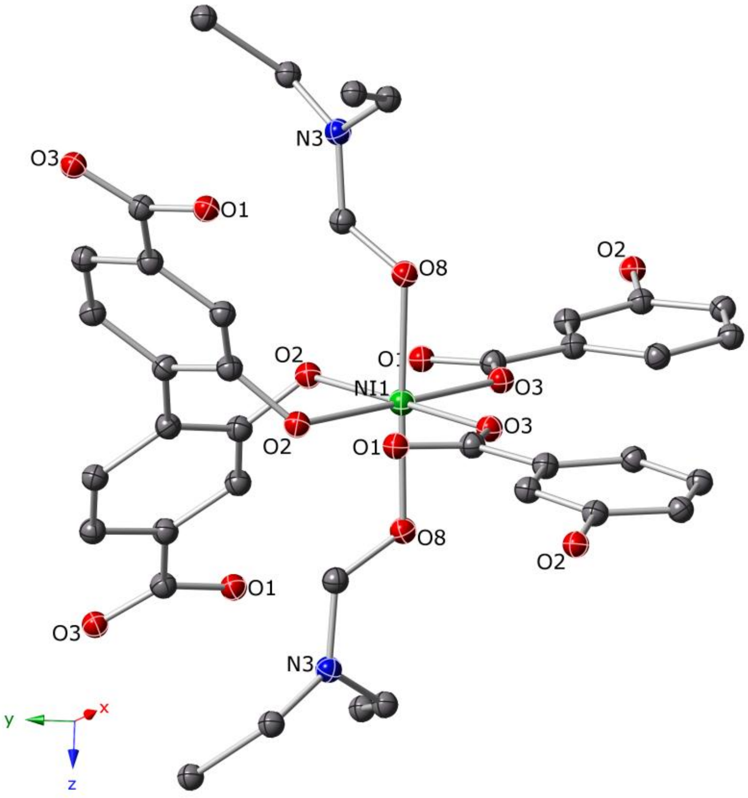

Figure S4.2. Coordination environment around the Ni(II) centre in **[Ni(H$_2$diol)(DEF)$_2$]**. Hydrogen atoms have been omitted for clarity.

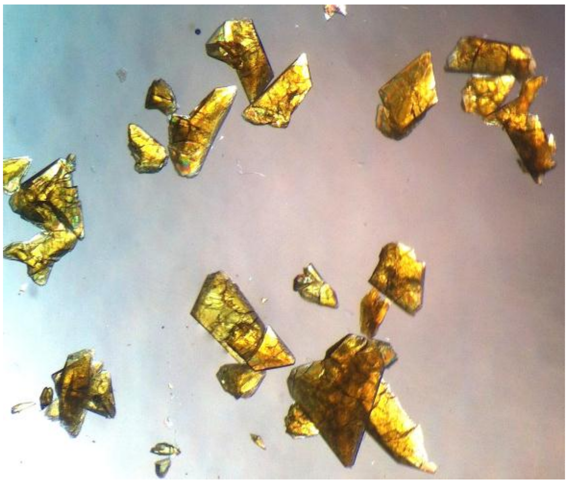

Figure S4.3. Crystals of **[Ni(H_2diol)]**. Images taken using a microscope camera at 5.0 x optical zoom.

Table S1. Crystal data and structure refinement for [Ni(H_2diol)(DMF)$_2$]·DMF.

Identification code	[Ni(H_2diol)(DMF)$_2$]·DMF	
Empirical formula	C20 H20 N2 Ni O8	
Formula weight	475.09	
Temperature	150(2) K	
Wavelength	0.71073 Å	
Crystal system	Trigonal	
Space Group	$P3_121$	
Unit cell dimensions	a = 17.2139(3) Å	α = 90°.
	b = 17.2139(3) Å	β = 90°
	c = 8.5240(5) Å	γ = 120°
Volume	2187.42(14) Å^3	
Z,	3	
Calculated density	1.082 Mg/m^3	
Absorption coefficient	0.701 mm^{-1}	
F(000)	738	
Crystal size	0.10 x 0.10 x 0.07 mm	
Theta range for data collection	2.73 to 26.98°	
Limiting indices	-21<=h<=21, -21<=k<=20, -10<=l<=10	
Reflections collected / unique	14078 / 3165 [$R_{(int)}$ = 0.0412]	
Completeness to theta = 26.98	99.8%	
Absorption correction	Semi-empirical from equivalents	
Max. and min. transmission	1.00000 and 0.57629	
Refinement method	Full-matrix least-squares on F^2	
Data / restraints / parameters	3165 / 0 / 141	
Goodness-of-fit on F^2	1.102	
Final R indices [I>2σ(I)]	R_1 = 0.0419, wR_2 = 0.1150	
R indices (all data)	R_1 = 0.0491, wR_2 = 0.1185	
Absolute structure parameter	-0.013(17)	
Largest diff. peak and hole	0.851 and -0.278 e.A^{-3}	

Table S2. Crystal data and structure refinement for $[\mathrm{Ni(H_2diol)(DEF)_2}]$·⅓DEF.

Identification code	$[\mathrm{Ni(H_2diol)(DEF)_2}]$·⅓DEF	
Empirical formula	C24 H28 N2 Ni O8	
Formula weight	531.19	
Temperature	150.0 K	
Wavelength	0.7107 A	
Crystal system, space group	Trigonal,	
Space group	$P\ 3_121$	
Unit cell dimensions	a = 17.3278(4) Å	α = 90°
	b = 17.3278(4) Å	β = 90°
	c = 9.1188(3) Å	γ = 120°
Volume	2371.13(11) A^3	
Z	3	
Calculated density	1.116 Mg/m^3	
Absorption coefficient	0.653 mm^{-1}	
F(000)	834	
Crystal size	0.10 x 0.08 x 0.08 mm	
Theta range for data collection	2.61 to 26.99 °.	
Limiting indices	-22<=h<=21, -21<=k<=22, -11<=l<=11	
Reflections collected / unique	16981 / 3456 [$R_{(int)}$ = 0.0536]	
Completeness to theta = 26.99	99.9 %	
Absorption correction	Semi-empirical from equivalents	
Max. and min. transmission	1.00000 and 0.82567	
Refinement method	Full-matrix least-squares on F^2	
Data / restraints / parameters	3456 / 8 / 154	
Goodness-of-fit on F^2	1.228	
Final R indices [$I>2\sigma(I)$]	R_1 = 0.0931, wR_2 = 0.2582	
R indices (all data)	R_1 = 0.0948, wR_2 = 0.2592	
Absolute structure parameter	0.00(1)	
Largest diff. peak and hole	1.518 and -1.830 $e.A^{-3}$	

iii. Powder X-ray diffraction

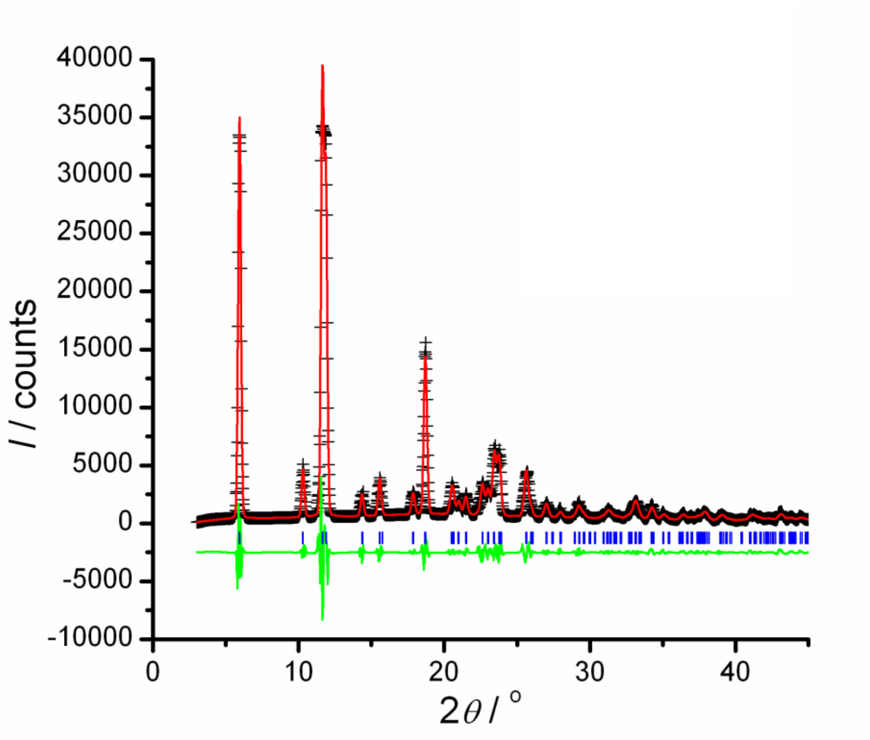

Figure S4.4. Le Bail refinement of **[Ni(H_2diol)(DMF)$_2$]** showing the experimental pattern (crosses), model (red), peak positions (blue) and difference plot (green).

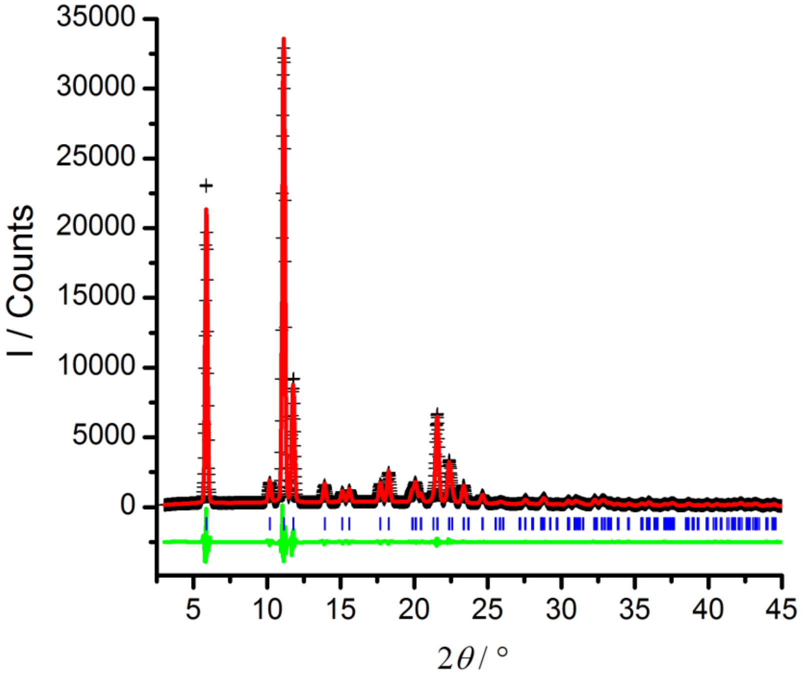

Figure S4.5. Le Bail refinement of **[Ni(H_2diol)(DEF)$_2$]** showing the experimental pattern (crosses), model (red), peak positions (blue) and difference plot (green).

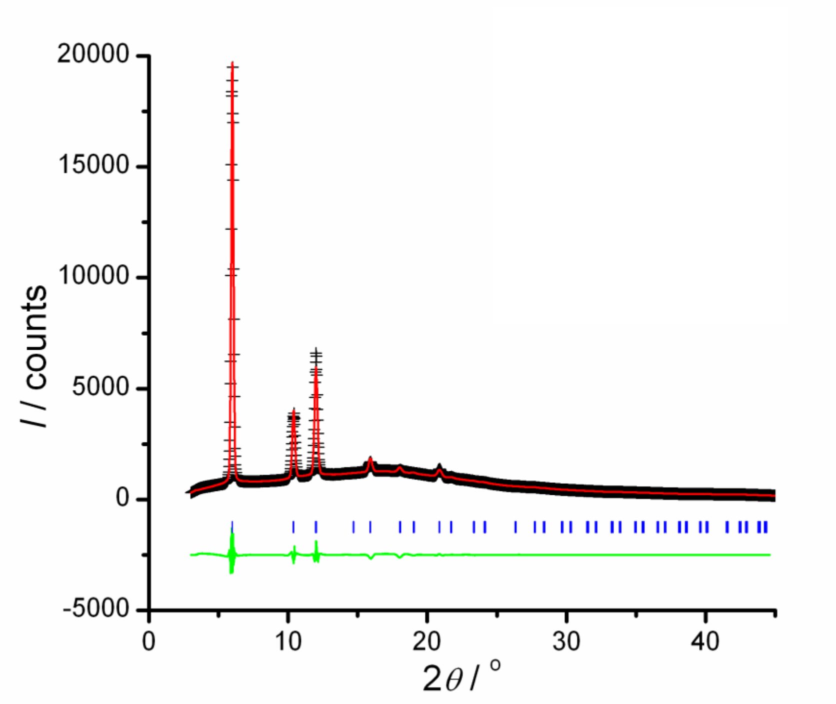

Figure S4.6. Le Bail refinement of **[Ni(H_2diol)]** showing the experimental pattern (crosses), model (red), peak positions (blue) and difference plot (green).

Table S3. Unit cell parameters calculated from Le Bail refinements of powder X-ray diffraction patterns.

	[Ni(H_2diol)(DMF)$_2$]	**[Ni(H_2diol)(DEF)$_2$]**	**[Ni(H_2diol)]**
Crystal System	hP	hP	hP
Space Group	$P3_121$	$P3_121$	$P3_221$
a- / b-axis (Å)	17.1362	17.3614	17.0239
c-axis (Å)	9.199	9.3559	8.5170
α = β (º)	90	90	90
γ (º)	120	120	120
Volume (Å^3)	2339.4	2442.2	2134.9
R_1	4.138	3.965	2.057
R_{wp}	6.046	5.781	3.322
GooF	0.086	2.731	0.990

5. Gas Adsorption

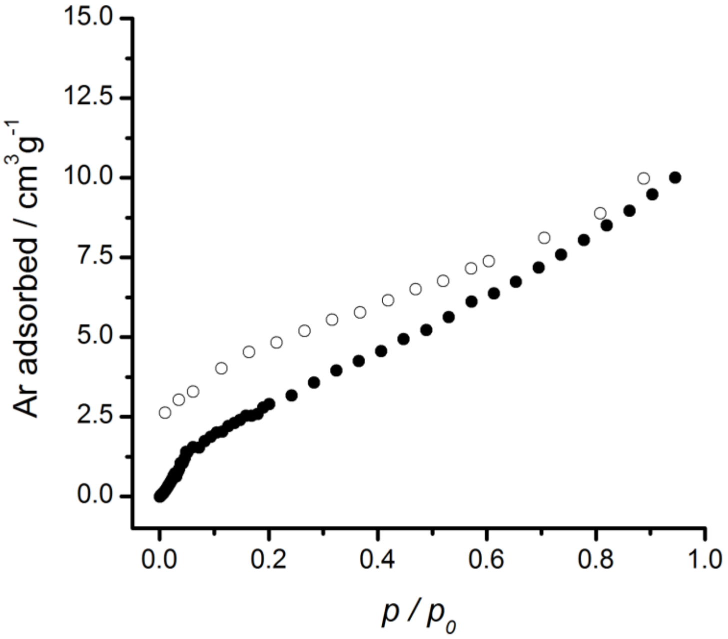

Figure S5.1. Ar adsorption isotherm for [**Ni(H_2diol)]** at 77K.

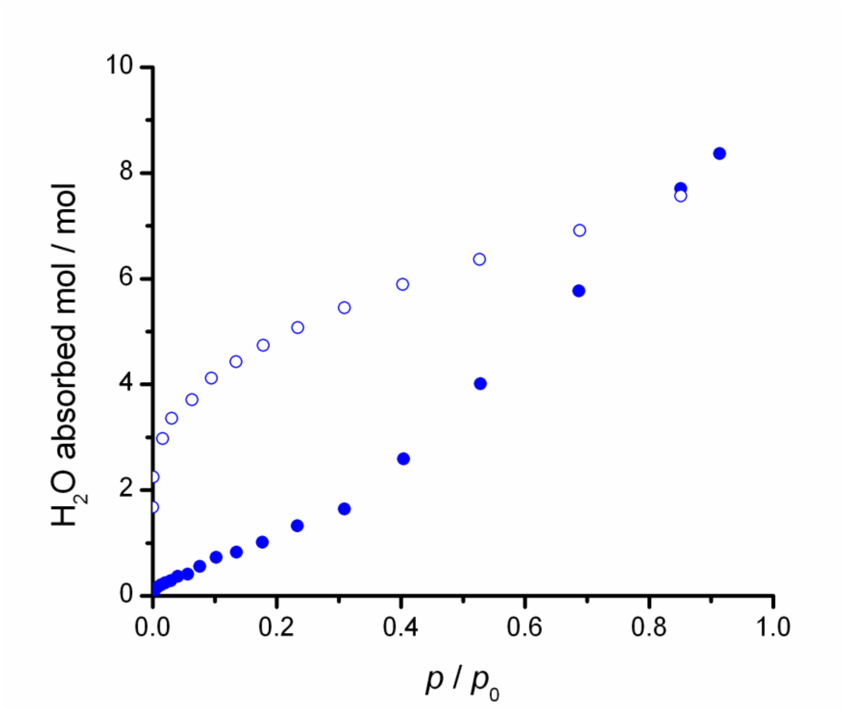

Figure S5.2. H_2O vapour isotherm for **[Ni(H_2diol)]** at 298K.

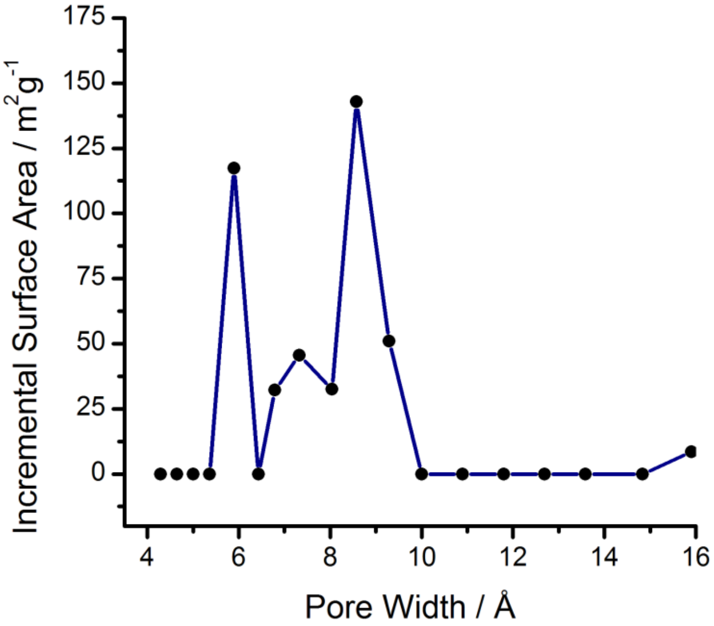

Figure S5.3. Pore size distribution of [**Ni(H_2diol)(DMF)$_2$]** from its N_2 isotherm at 77 K.

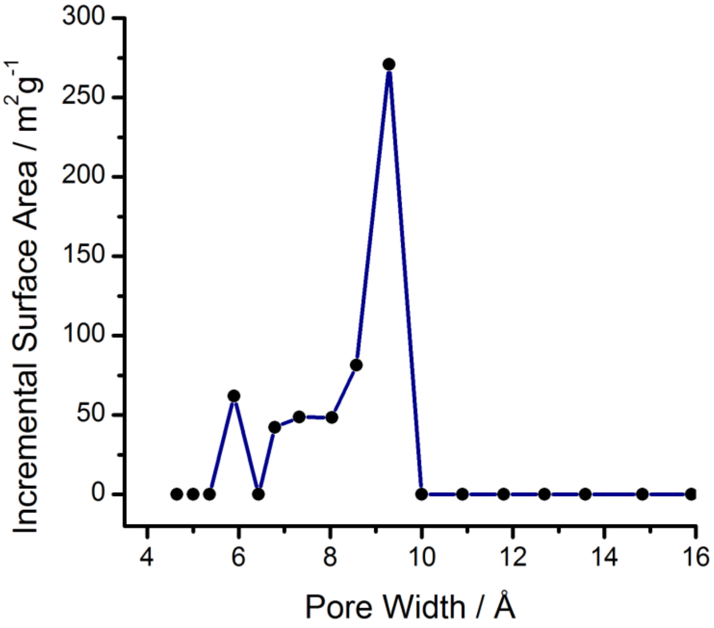

Figure S5.4. Pore size distribution of **[Ni(H_2diol)(DEF)$_2$]** from its N_2 isotherm at 77 K.

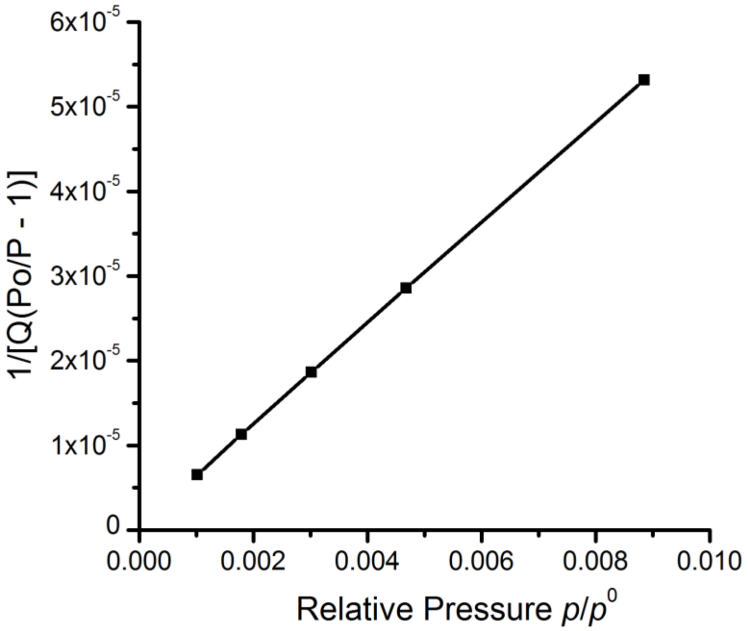

Figure S5.5. BET plot of **[Ni(H_2diol)(DMF)$_2$]** from N_2 isotherm at 77 K.

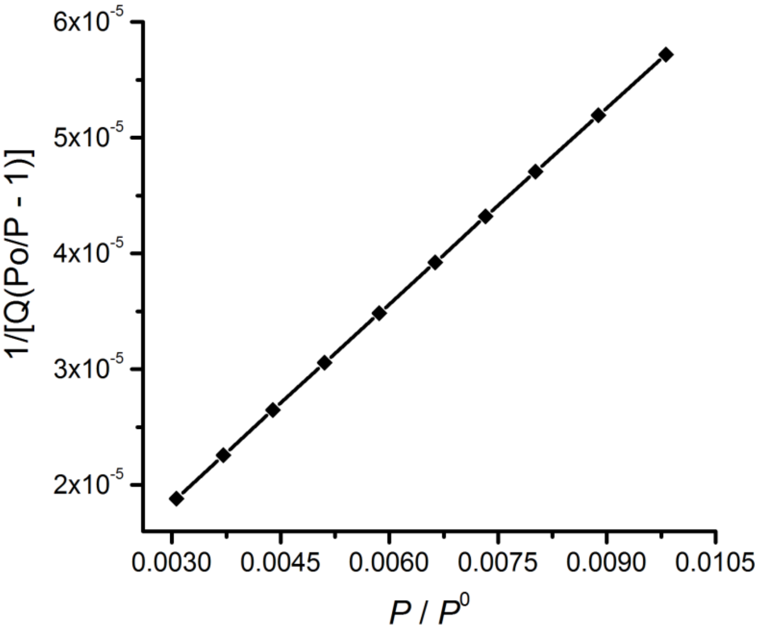

Figure S5.6. BET plot of **[Ni(H_2diol)(DEF)$_2$]** from N_2 isotherm at 77 K.

Table S4. BET statistics from N_2 isotherms collected at 77K.

	$[Ni(H_2diol)(DMF)_2]$	**$[Ni(H_2diol)(DEF)_2]$**
BET Surface Area	732.9 ± 2.5 m^2/g	766.6 ± 1.0 m^2/g
Slope	0.005939 ± 0.000021 g/cm^3 STP	0.005677 ± 0.000008 g/cm^3 STP
Y-Intercept	0.000001 ± 0.000000 g/cm^3 STP	0.000002 ± 0.000000 g/cm^3 STP
C	9013.0	3703.3
Qm	168.3 cm^3/g STP	176.1 cm^3/g STP
Correlation Coefficient	0.9999821	0.9999927

6. Structural Properties

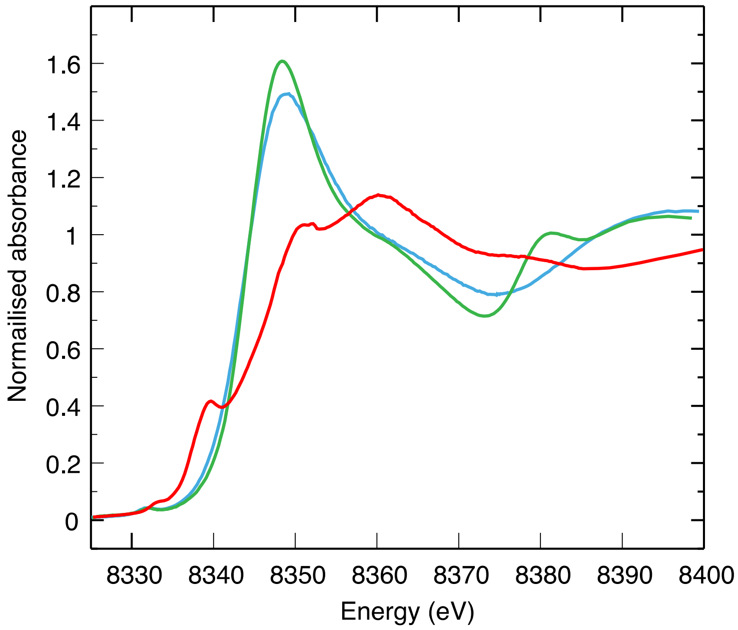

Figure S6.1. Ni K-edge XANES spectra of octahedral **[Ni(H_2diol)(DMF)$_2$]** (green), distorted tetrahedral **[Ni(H_2diol)]** (blue) and a reference compound – square-planar [Ni(II)salen] (red).

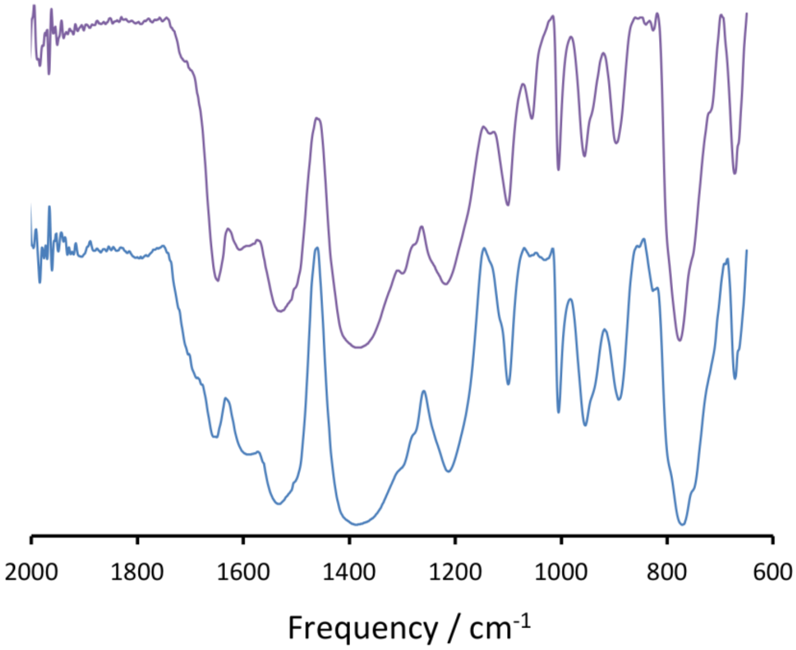

Figure S6.2. Infrared spectra of **[Ni(H_2diol)(DMF)$_2$]·DMF** (purple) and **[Ni(H_2diol)]** (blue).

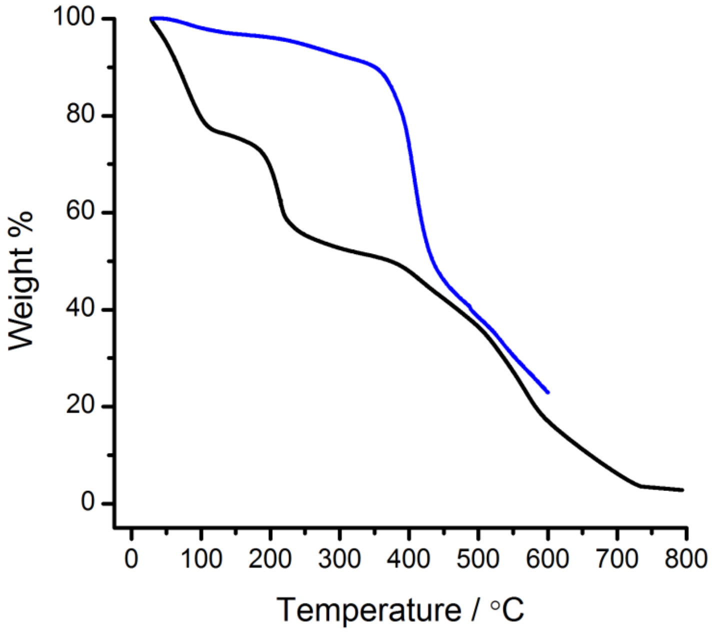

Figure S6.3. Thermogravimmetric analysis (TGA) of **[Ni(H_2diol)(DMF)$_2$]·DMF** (black) and **[Ni(H_2diol)]** (blue).

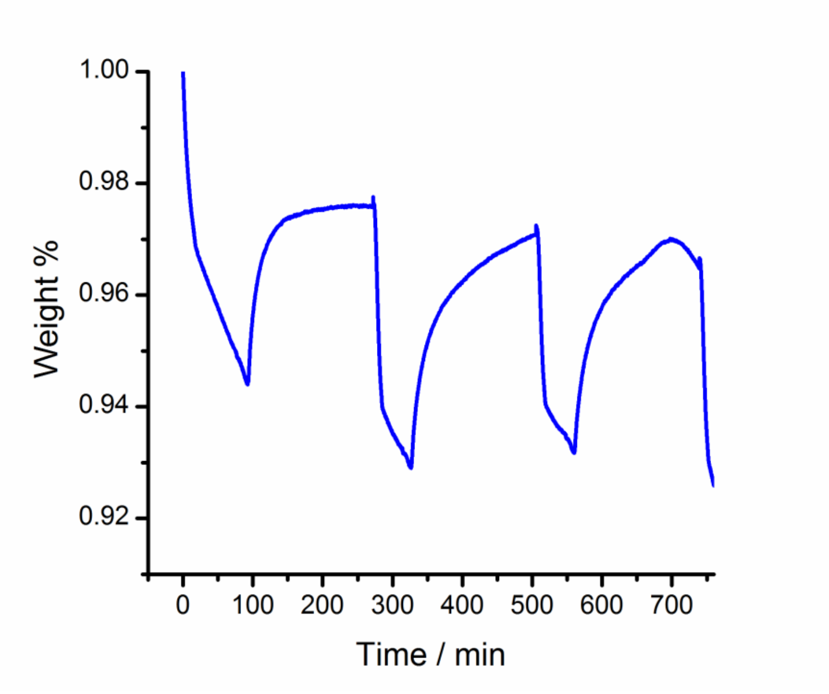

Figure S6.4. TGA analysis of water cycling for [**Ni(H_2diol)(DMF)$_2$]** under the following conditions: heating phase – 200ºC under N_2 flow (20 L/min); cooling phase – 40ºC under Ar flow (20 L/min) passed through a H_2O bubbler at room temperature.

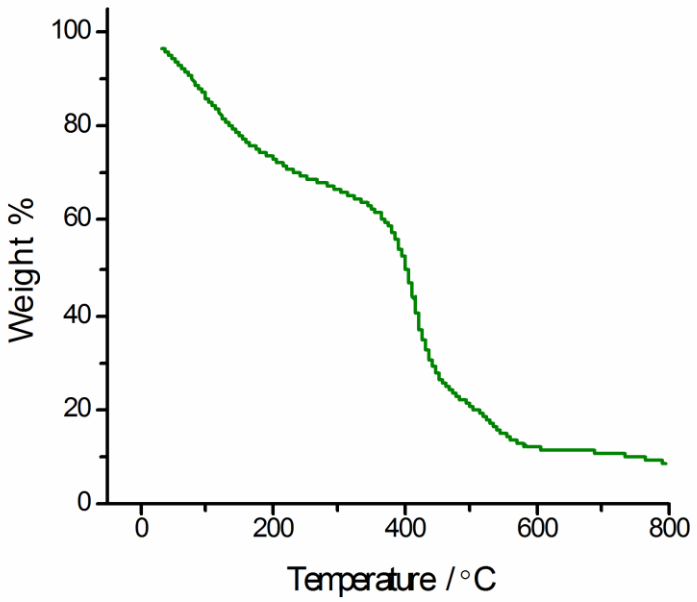

Figure S6.5. TGA analysis of [**Ni(H_2diol)(DMF)$_2$]** that had been soaked in MeOH, heated at 100ºC to produce [**Ni(H_2diol)]**, followed by attempted resolvation with DMF (soaked for 48 hrs). The TGA shows no loss of DMF at ~200ºC (as seen in **Figure S6.3** for **[Ni(H_2diol)(DMF)$_2$]·DMF**) indicating a lack of resolvation by DMF onto the Ni centre.

7. References

(1) S. Brunauer; P. H. Emmett, E. Teller, *J. Am. Chem. Soc.* 1938, **60**, 309.

(2) K. S. Walton, R. Q. Snurr, *J. Am. Chem. Soc*., 2007, **129**, 8552.

(3) a) D. Rankine, A. Avellaneda, M. H. Hill, C. J. Doonan, C. J. Sumby, *Chem. Comm.*, 2012, **48**, 10328; b) M. Rizzacasa, M. V. Sargent, *Aust. J. Chem.*, 1988, **41**, 1087.

(4) G. M. Sheldrick, *Acta Cryst.* , 1990, **A46**, 467.

(5) Sheldrick, G. M., In "Crystallographic Computing 3", Ed. G. M. Sheldrick, C. Kruger and R. Goddard, Oxford University Press. pp. 175-189, 1985.

(6) L. J. Farrugia, *J. Appl. Cryst.*, 1999, **32**, 837.